Published in final edited form as:
J Comp Neurol. 2009 January 20; 512(3): 419–431. doi:10.1002/cne.21880.

Subcellular targeting of kappa-opioid receptors in the rat nucleus locus coeruleus

B. A. S. Reyes, **Charles Chavkin***, and **E. J. Van Bockstaele**

Department of Neurosurgery, Thomas Jefferson University, Farber Institute for Neurosciences, Philadelphia, PA 19107

* Department of Pharmacology, University of Washington, Seattle, WA 98195

Abstract

The dynorphin (DYN)-kappa opioid receptor (κOR) system has been implicated in stress modulation, depression and relapse to drug-seeking behaviors. Previous anatomical and physiological data have indicated that the noradrenergic nucleus locus coeruleus (LC) is one site at which DYN may contribute to these effects. Using light microscopy, immunofluorescence and electron microscopy, the present study investigated the cellular substrates for pre- and postsynaptic interactions of κOR in the LC. Dual immunocytochemical labeling for κOR and tyrosine hydroxylase (TH) or κOR and preprodynorphin (ppDYN) was examined in the same section of tissue. Light microscopic analysis revealed prominent κOR immunoreactivity in the nuclear core of the LC and in the peri-coerulear region where noradrenergic dendrites extend. Fluorescence and electron microscopy revealed κOR immunoreactivity within TH-immunoreactive somata and dendrites in the LC as well as localized to ppDYN-immunoreactive processes. In sections processed for κOR and TH, approximately 29% (200/688) of the κOR-containing axon terminals identified targeted TH-containing profiles. Approximately 49% (98/200) of the κOR-labeled axon terminals formed asymmetric synapses with TH-labeled dendrites. Sections processed for κOR and ppDYN showed that, of the axon terminals exhibiting κOR, 47% (223/477) also exhibited ppDYN. These findings indicate that κORs are poised to modulate LC activity by their localization to somata and dendrites. Furthermore, κORs are strategically localized to presynaptically modulate DYN afferent input to catecholamine-containing neurons in the LC. These data add to the growing literature showing that κORs can modulate diverse afferent signaling to the LC.

Keywords

kappa-opioid receptors; dynorphin; locus coeruleus; tyrosine hydroxylase; electron microscopy

Introduction

Dynorphin (DYN), a kappa opioid receptor (κOR) ligand, is a potent endogenous opioid peptide that is widely distributed throughout the brain (Elde and Hokfelt, 1993; Fallon and Leslie, 1986; Goldstein and Ghazarossian, 1980; Hollt et al., 1980; Khachaturian et al., 1982; Watson et al., 1982; Watson et al., 1983) and is implicated in stress modulation, depression and relapse to drug-seeking behaviors (Schenk et al., 1999; Shirayama et al.,

*Corresponding Author: Beverly A. S. Reyes, PhD, Department of Neurosurgery, Farber Institute for Neurosciences, Thomas Jefferson University, 900 Walnut Street, Suite 400, Philadelphia, PA 19107, Voice: (215) 503-5268, FAX: (215) 955-7921, e-mail: bsr103@jefferson.edu.
Name of Associate Editor: Paul E. Sawchenko, PhD

2004). While others have demonstrated that κOR mRNA and protein are expressed in the locus coeruleus (LC; DePaoli et al., 1994; Mansour et al., 1994b), we have provided ultrastructural evidence that DYN axon terminals form primarily asymmetric synaptic specializations with noradrenergic dendrites in the LC (Barr and Van Bockstaele, 2005; Reyes et al., 2008; Reyes et al., 2007) and physiological evidence for DYN regulation of afferent inputs to the LC (Kreibich et al., 2008). We have also shown that DYN is co-localized with glutamate (Barr and Van Bockstaele, 2005) and other stress-related peptides such corticotropin releasing factor (CRF; Reyes et al., 2008).

DYN levels are increased in limbic brain regions during stress and depression (Shirayama et al., 2004). Stress has been shown to induce DYN release and subsequent activation of κOR (Mague et al., 2003; McLaughlin et al., 2003). In humans, κOR agonists cause the manifestation of the dysphoric component of stress (Pfeiffer et al., 1986; Roth et al., 2002). While stimulation of the brain κORs may trigger certain signs of depression (Todtenkopf et al., 2004), κOR antagonists demonstrate antidepressant-like effects (Mague et al., 2003). Meanwhile, intracellular physiological studies have shown that application of κOR agonists (U50488) *in vitro* produces a concentration-dependent depression of the excitatory postsynaptic potential evoked by electrical stimulation of afferent inputs to LC neurons (McFadzean et al., 1987). These findings were extended by Pinnock (Pinnock, 1992) who demonstrated that the κOR agonist (CI-977) causes a depression of evoked postsynaptic potentials on LC neurons and the depression remained in the presence of a glutamate antagonist (Pinnock, 1992).

Despite these pharmacological and physiological studies, the cellular substrate of interaction between κOR and catecholamine-containing neurons in LC has not been shown. Considering that the LC contains the largest cluster of noradrenergic neurons in the brain (Foote et al., 1983; Waterhouse et al., 1993) and serves as the principal source of norepinephrine in the brain (Aston-Jones et al., 1984; McCormick et al., 1991), understanding the anatomical substrates underlying potential interactions of κOR with noradrenergic neurons is important. LC neurons play a vital role in global brain functions such as emotion, vigilance (Aston-Jones et al., 1984), memory and adaptive responses to stress (Aston-Jones and Bloom, 1981; Aston-Jones et al., 1991). In addition, LC neurons respond to autonomic influences and discharge in parallel with peripheral sympathetic nerves (Elam et al., 1985; Elam et al., 1986; Elam et al., 1984; Svensson, 1987a; Svensson, 1987b; Valentino et al., 1998; Valentino et al., 1983), and are implicated in autonomic functions (Lechner et al., 1997; Miyawaki et al., 1991; Morilak et al., 1987a; Morilak et al., 1987b; Murase et al., 1993).

Therefore, in the present study, light microscopy, immunofluorescence and immunoelectron microscopy were used to identify the anatomical distribution of κOR in LC. Further, the localization of κOR with respect to DYN was also examined to determine whether κORs act as autoreceptors in this region. For semi-quantitative analysis of associations between κOR and TH or preprodynorphin (DYN), immunoelectron microscopic dual-immunolabeling procedure was carried out. Specifically, we employed immunogold-silver labeling of κOR and immunoperoxidase labeling of TH or ppDYN in the same section of tissue in adult rat LC.

MATERIALS AND METHODS

Animals

Ten adult male Sprague-Dawley rats (250–300 g; Harlan Sprague-Dawley, Inc., Indianapolis, IN) were used in the present study. The rats were housed 2–3 per cage on a 12-h light schedule in a temperature controlled (20 °C) colony room. They were given standard

rat chow and water. All efforts were made to utilize only the minimum number of animals necessary to produce reliable scientific data and experiments were designed to minimize any animal distress. The procedures were approved by the Institutional Animal Care and Use Committee of Thomas Jefferson University and conformed to *NIH guide for care and use of laboratory animals*.

Specificity of antisera

In the present study, an affinity-purified polyclonal antibody raised against the carboxyl terminal 15 amino acids of the cloned rat κOR (RDVGGMNKPV) was generated in rabbit. Characterization of this antibody was conducted in previous studies (Drake et al., 1996) and additional specificity tests were conducted in this study. It has been previously characterized and its specificity was confirmed by Western blotting, enzyme-linked immunosorbent assays and κOR immunolabeling in Xenopus oocytes (Drake et al., 1996). Using Western blot analysis, the κOR antibody recognized two bands of proteins with approximate molecular weights of 97,000 and 66,000 (Drake et al., 1996). Incubating serial sections in primary κOR antiserum preabsorbed with 10 μM antigenic peptide showed no immunoreactivity. Blots incubated with 1.5 μg/ml of affinity-purified κOR antiserum preincubated with antigenic peptide did not show any bands. The κOR antibody specificity was also demonstrated by κOR immunoreactivity in the forebrain and pons (Drake et al., 1996) and spinal cord (Wang et al., 2007). We also examined κOR specificity by using HEK293 cells transiently transfected with pcDNA3-FLAG-rat κOR and double labeled with the M2 monoclonal antibody against FLAG followed by AlexaFluor 488-conjugated goat anti-mouse IgG and κOR followed by Texas Red-conjugated goat anti-rabbit IgG. A consistent identical staining was observed indicating that the antibody used recognizes κOR.

The immunogen for mouse monoclonal antiserum was raised against denatured TH from rat pheochromocytoma, labels a single band at approximately 62kD corresponding to TH, and does not cross-react with dopamine-β-hydroxylase, dihydropterdine reductase, phenylethanolamine-N-methyltransferase, phenylalanine hydroxylase or tryptophan hydroxylase. The antibody has wide species cross-reactivity. The specificity of the TH antibody has been examined by preabsorption of the antibody with a high concentration of TH (Van Bockstaele and Pickel, 1993). Omission of the primary antibody abolished any detectable immunoreactivity (Reyes et al., 2007).

The antiserum against residues 235-248 (SQENPNTYSEDLDV) of rat ppDYN was generated in guinea pig (Arvidsson et al., 1995). The specificity of ppDYN antiserum was tested by absorption controls with the cognate peptides (Arvidsson et al., 1995; Reyes et al., 2007). We have shown that preabsorption of ppDYN with the antigenic peptide at 1 μM blocked the immunoreactivity in regions known to express DYN (hippocampus, spinal cord; Reyes et al., 2007). This is in agreement with others showing that DYN staining in rat brain tissue was blocked at peptide concentrations of 0.1 to 1 μM (Arvidsson et al., 1995). The distribution of ppDYN immunoreactivity was consistent with the localization of DYN immunoreactivity seen in other studies that examined LC (Elde and Hokfelt, 1993). Tissue sections processed in the absence of primary antibody did not exhibit any detectable immunoreactivity (Reyes et al., 2007).

Immunofluorescence

Five rats were deeply anesthetized with sodium pentobarbital (80 mg/kg; Ovation Pharmaceuticals, Inc., Deerfield, IL) and transcardially perfused through the ascending aorta with 500 ml of 4% formaldehyde in 0.1 M phosphate buffer (PB; pH 7.4). Brains were removed, blocked, post fixed in 4% formaldehyde overnight at 4°C, and stored in 30% sucrose solution in 0.1 M PB containing sodium azide at 4°C for few days. The rat brain was

frozen using Tissue Freezing Medium (Triangle Biomedical Science, Durham, NC). Frozen 30 μm-thick sections were cut in the coronal plane using a freezing microtome (Micron HM550 cryostat; Richard-Allan Scientific, Kalamazoo, MI) and collected in 0.1 M PB. Sections were placed for 30 min in 1% sodium borohydride in 0.1 M PB to reduce amine-aldehyde compounds. The tissue sections were then incubated in 0.5% bovine serum albumin (BSA) and 0.25% Triton X-100 in 0.1 M tris-buffered saline (TBS; pH 7.6) for 30 min. Thorough rinses in 0.1 M TBS were done following incubation. Subsequently, sections were incubated in rabbit anti- κOR at 1:500 or rabbit anti- κOR at 1:500 and mouse anti-TH (Immunostar Inc., Hudson, WI, USA) at 1:1,000 in 0.1% BSA and 0.25% Triton X-100 in 0.1M TBS. Incubation time was 15–18 h in a rotary shaker at room temperature. Sections were then washed in 0.1 M TBS and incubated in a secondary antibody cocktail containing fluorescein isothiocyanate (FITC) donkey anti-rabbit (1:200; Jackson ImmunoResearch Laboratories Inc., West Grove, PA, USA) and tetramethyl rhodamine isothiocyanate (TRITC) donkey anti-mouse (1:200; Jackson ImmunoResearch) antibodies prepared in 0.1 % BSA and 0.25% Triton X-100 in 0.1 M TBS for 2 h in the dark on a rotary shaker.

Sections processed for κOR and preprodynorphin (ppDYN) were incubated in a cocktail containing rabbit anti- κOR at 1:500 and guinea-pig anti-ppDYN at 1:16,000 (kindly provided by Dr. Robert Elde, University of Minnesota, MN). Incubation time was 15–18 h in a rotary shaker at room temperature. Sections were then washed in 0.1 M TBS and incubated in a secondary antibody cocktail containing TRITC donkey anti-rabbit (1:100; Jackson ImmunoResearch Laboratories Inc.) and FITC donkey anti-guinea pig (1:100; Jackson ImmunoResearch Laboratories Inc.) prepared in 0.1 % BSA and 0.25% Triton X-100 in 0.1 M TBS for 2 h in the dark on a rotary shaker.

The tissue sections were washed thoroughly in 0.1 M TBS following incubation with the secondary antibodies, were then mounted on slides and allowed to dry in complete darkness. The slides were coverslipped using DPX (Sigma-Aldrich Inc., St. Louis, MO, USA) and immediately examined using a Leica DMRBE microscope (Leica Microsystems, Wetzlar, Germany) equipped for fluorescence with rhodamine and fluorescein filters. Images were captured using Spot Advance software (Diagnostic Instruments Inc., Sterling Heights, MI).

Immunoelectron microscopy

Following the standard protocols for immunoelectron microscopy (Chan et al., 1990), five rats were used. Briefly, rats were deeply anesthetized with sodium pentobarbital (80 mg/kg) and perfused transcardially through the ascending aorta with 10 ml heparinized saline followed with 50 ml of 3.75% acrolein (Electron Microscopy Sciences, Fort Washington, PA, USA), and 200 ml of 2% formaldehyde in 0.1 M PB (pH 7.4). The brains were removed immediately after perfusion fixation, sectioned into 1–3 mm coronal slices and postfixed in the same fixative overnight at 4°C. Sections were cut in the coronal plane at a setting of 40 μm using a Vibratome (Technical Product International, St. Louis, MO) and collected into 0.1 M PB.

Sections through the rostrocaudal extent of the LC were processed for electron microscopic analysis of κOR, κOR and TH or κOR and ppDYN in the same section. Sections containing the LC were processed following the protocol described earlier for immunofluorescence except that Triton X-100 was not added to the solution for antibody incubation. Tissue sections were incubated in rabbit anti- κOR (1:500) or in primary antibody cocktail of rabbit anti- κOR (1:500) and mouse anti-TH (1:1,000; Immunostar Inc.) or guinea pig anti-ppDYN (1:16,000) for 15–18 h at room temperature. In singly-labeled sections, κOR immunoreactivity was detected using immunoperoxidase. In both set of sections that were dual-labeled for κOR and TH or ppDYN, immunoperoxidase labeling was used to identify TH or ppDYN immunoreactivity while immunogold-silver labeling was used to identify

κOR immunoreactivity. The following day tissue sections were rinsed three times in 0.1 M TBS and incubated in biotinylated donkey anti-mouse (1:400; Vector Laboratories, Burlingame, CA) or biotinylated donkey anti-guinea pig (1:400; Vector Laboratories) for 30 min followed by rinses in 0.1 M TBS. Subsequently, a 30-minute incubation of avidin-biotin complex (Vector Laboratories) followed. For all incubations and washes, sections were continuously agitated with a rotary shaker. TH or ppDYN was visualized by a 4-min reaction in 22 mg of 3,3′-diaminobenzidine (Sigma-Aldrich Inc., St. Louis, MO) and 10 μl of 30% hydrogen peroxide in 100 ml of 0.1 M TBS. Additionally, some tissue sections incubated in rabbit anti- κOR were also processed in parallel for immunoperoxidase labeling except that biotinylated donkey anti-rabbit antibody was used. Immunoperoxidase labeled sections for κOR were mounted, dehydrated in an ascending series of ethanol and coverslipped for light microscopic analysis of κOR immunoreactivity.

For gold-silver localization of κOR, sections were rinsed three times with 0.1 M TBS, followed by rinses with 0.1 M PB and 0.01 M phosphate buffered saline (PBS; pH 7.4). Sections were then incubated in a 0.2% gelatin-PBS and 0.8% BSA buffer for 10 min and followed by incubation in goat anti-rabbit IgG conjugate in 1 nm gold particles (Amersham Bioscience Corp., Piscataway, NJ, USA) at room temperature for 2 h. Sections were then rinsed in buffer containing the same concentration of gelatin and BSA as above. Following rinses with 0.01 M PBS, sections were then incubated in 2% glutaraldehyde (Electron Microscopy Sciences) in 0.01 M PBS for 10 min. This procedure was followed by washes in 0.01 M PBS and 0.2 M sodium citrate buffer (pH 7.4). A silver enhancement kit (Amersham Bioscience Corp.) was used for silver intensification of the gold particles. The optimal times for silver enhancement were determined by empirical observation for each experiment and ranged between 8 and 10 min. To avoid bias in labeling, some tissue sections incubated for κOR + TH were reversed labeled such that κOR was labeled for immunoperoxidase and TH was labeled with immunogold-silver. Following intensification, tissue sections were rinsed in 0.2 M citrate buffer and 0.1 M PB, and incubated in 2% osmium tetroxide (Electron Microscopy Sciences) in 0.1 M PB for 1 h, washed in 0.1 M PB, dehydrated in an ascending series of ethanol followed by propylene oxide and flat embedded in Epon 812 (Electron Microscopy Sciences; (Leranth and Pickel, 1989).

Thin sections of approximately 50–100 nm in thickness were cut with a diamond knife (Diatome-US, Fort Washington, PA, USA) using a Leica Ultracut (Leica Microsystems, Wetzlar, Germany). Captured images of selected sections were compared with captured light microscopic images of the block face before sectioning. Sections were collected on copper mesh grids, examined with an electron microscope (Morgagni, Fei Company, Hillsboro,OR, USA) and digital images were captured using the AMT advantage HR/HR-B CCD camera system (Advance Microscopy Techniques Corp., Danvers, MA, USA). Figures were assembled and adjusted for brightness and contrast in Adobe Photoshop.

Control and data analysis

Some sections were processed in parallel with the rest of the procedures identical but one of the primary antisera was omitted. Sections processed in the absence of primary antibody did not exhibit immunoreactivity. To evaluate cross-reactivity of labeling of the primary antiserum by secondary antisera, some sections were processed for dual labeling with omission of one of the primary antisera. Tissue sections were taken from five rats with the good preservation of ultrastructural morphology and with clearly apparent immunocytochemical labeling. At least 10 grids containing 5 to 10 thin sections each were collected from at least three plastic-embedded sections of the LC from each animal. For quantification of immunolabeled profiles before embedding for electron microscopy, we have observed that the collection of sections only from the surface of the section minimizes artifacts that may be associated with incomplete penetration of antisera. The analysis of

tissue sections collected at the plastic-tissue interface ensured that both markers were detectable in all sections used for analysis (Chan et al., 1990). Selective immunogold-silver-labeled profiles were identified by the presence, in single thin sections of at least 2–3 silver grains in a cellular profile, otherwise a cellular profile in adjacent thin section was designated lacking detectable immunoreactivity. As observed in low magnification electron micrographs, background labeling in the neuropil, deemed spurious, was not commonly encountered.

The cellular elements were identified based on the description of Peters and colleagues (Peters and Palay, 1996). Somata contained a nucleus, Golgi apparatus and smooth endoplasmic reticulum. Proximal dendrites contained endoplasmic reticulum, were postsynaptic to axon terminals and were larger than 0.7 μm in diameter. A terminal was considered to form a synapse if it showed a junctional complex, a restricted zone of parallel membranes with slight enlargement of the intercellular space, and/or associated with postsynaptic thickening. Asymmetric synapses were identified by thick postsynaptic densities (Gray's type I; Gray, 1959), in contrast, symmetric synapses had thin densities (Gray's type II; Gray, 1959) both pre- and postsynaptically. The term "undefined" synaptic contact was used to denote parallel membrane association of an axon terminal plasma membrane juxtaposed to that of a dendrite or soma which lacked recognizable membrane specializations in the plane of section analyzed, and with no intervening glial processes.

Identification of gold-silver labeling in profiles

Using electron microscopy in all rats analyzed, immunogold-silver labeling for κOR was identified in axon terminals and dendrites, sometimes in unmyelinated axons in the LC. As observed in low magnification electron micrographs, background labeling in the neuropil, deemed spurious, was not commonly encountered. Therefore, selective immunogold-silver labeled profiles were identified by the presence, in single thin sections, of at least two-three immunogold-silver particles within a cellular compartment. Whenever possible, the more lightly labeled axonal labeling for κOR was confirmed by detection in at least two serial sections. The criterion of three gold particles as indicative of κOR labeling is conservative and may have led to an underestimation of the number of κOR-labeled profiles. Another factor that may have led to the underestimation of labeled profiles is the limitation of immunocytochemical methods to detect trace amounts of κOR. Moreover, unbiased stereological methods were not used for counting labeled profiles, and the results of the numerical analysis can only be considered to be an estimate of the numbers of synapses and labeled profiles.

RESULTS

Immunocytochemical labeling of κOR and TH in the LC

The distribution of κORs in the LC was assessed using immunoperoxidase labeling of κOR alone as well as using dual immunofluorescence labeling of κOR and TH. A representative photomicrograph of immunoperoxidase labeling for κOR can be seen in Figure 1A. Immunoperoxidase labeling for κOR exhibited a punctate pattern of immunoreactivity throughout the rostro-caudal extent of the LC (Fig. 1A). Within the LC, κOR immunoreactivity was homogeneously distributed within the core of the LC as well as in the peri-coerulear (peri-LC) area. The core of the LC contains abundant TH-labeled perikarya (Bajic et al., 2000; Shipley et al., 1996) whereas the peri-LC is more enriched with TH-labeled dendrites (Shipley et al., 1996; Van Bockstaele et al., 1996). Within the core of the LC, κOR immunolabeling was localized to somata, dendrites and processes resembling axonal profiles (Fig. 1A1 and 1A2). Within the peri-LC, κOR immunolabeing was primarily localized to varicose processes resembling axons and terminals (Fig. 1A).

Using immunofluorescence labeling, κOR overlapped with, and was contained in, TH-immunolabeled somata and dendrites (Fig. 1B,D). κOR-immunoreactive processes were punctate in nature and could be seen to overlap TH-labeled somata and dendrites (Fig. 1B–D) in the core of the LC (Fig. 1B–D). In this region, TH-labeled somata also contained κOR immunoreactivity as seen in Figure 1D.

Immunofluorescence labeling of κOR and ppDYN in the LC

Immunohistochemical labeling for κOR and ppDYN was conducted in the same section of tissue through the LC region (Fig. 2A–F). Consistent with our recent report (Reyes et al., 2007), ppDYN immunoreactivity was detectable in both the core of the LC (Fig. 2B,C) that contains primarily noradrenergic somata and the peri-LC area that is enriched with noradrenergic dendrites (Fig. 2E,F). Within the core of the LC, ppDYN-immunolabeling showed a punctate, diffuse distribution (Fig. 2B), whereas in the peri-LC where noradrenergic dendrites extend, a prominent plexus of ppDYN fiber could be discerned (Fig. 2E). Using immunofluorescence, κOR immunolabeling showed a similar pattern as that found for peroxidase labeling with punctate immunolabeling in the core (Fig. 2A) and peri-LC (Fig. 2D) areas. Processes dually labeled for κOR and ppDYN were distributed throughout both the core (Fig. 2C) and peri-LC (Fig. 2F).

Ultrastructural analysis of κOR and TH

Using immunogold-silver (Fig. 3A–C) or immunoperoxidase detection methods (Fig. 3D), κOR immunoreactivity was identified in both pre- (Fig. 3A–D, 6A) and post-synaptic (Fig. 4A–D, 6B) cellular profiles. κOR immunoreactivity was localized to axon terminals (Fig. 3A–D) as well as diffusely distributed in dendrites (Fig. 4A–D) and somata (Fig. 6B). κOR immunogold-silver particles were distributed on the plasma membrane (Fig. 3A,C, 4A–D, 6B) as well as in the cytoplasmic compartments (Figure 3B–D, 4B–D). When κOR was found on the plasma membrane it was usually located along the intracellular face of plasma membranes which is in congruence with the position of the epitope that the κOR antibody recognizes in the C-terminal domain of the receptor. When κOR was found intracellularly, it was associated with intracellular structures including endosomes and vesicle-like structures, and it was also dispersed within the cytoplasmic compartment.

Of 1,061 κOR-immunoreactive profiles examined from five rats, 68% (718/1,061) of κOR-labeling was localized in axon terminals and 32% (342/1,061) was identified in dendrites and somata. Axon terminals with κOR immunoreactivity contained heterogeneous types of synaptic vesicles and were unmyelinated. κOR-labeled dendrites usually contained endoplasmic reticulum and were postsynaptic to axon terminals.

Semi-quantitative analysis of immunogold-silver labeling of κOR and immunoperoxidase labeling for TH showed that κOR-labeled axon terminals frequently formed synaptic specializations with TH-labeled dendrites. Out of 688 κOR-labeled axon terminals sampled, 29% (200/688) targeted TH-labeled dendrites. Out of 200 profiles, 61.5% (123/200) formed synapses (Fig. 3C–D) with TH-labeled dendrites while 38.5% (55/200) did not form recognizable synaptic specializations (Fig. 3B) in the plane of section analyzed. Of the 200 distinguishable synapses, 49% (98/200) were of the asymmetric type (Fig. 3C–D) while 11% (22/200) were of the symmetric type synapse (Fig. 5B) and 40% (80/200) did not show recognizable synaptic associations (Fig. 3B) that could be unequivocally classified as Type I or Type II. κOR axon terminals targeting TH- labeled dendrites also contained dense core vesicles (Fig. 3C–D) and sometimes were surrounded by astrocytic processes (Fig. 3C–D).

κOR and TH immunolabeling in the same dendritic profiles was also observed (Fig. 4A–D). Dendrites showing both κOR and TH immunoreactivities mostly received asymmetric

synapses from unlabeled axon terminals (Fig. 4A, D). Some dendrites exhibiting both κOR and TH immunolabeling did not receive any recognizable synaptic specializations from axon terminals in the plane of section examined (Fig. 4C). In addition, some κOR- and TH-immunolabeled dendrites were enveloped with astrocytic processes (Fig. 4B–D).

Ultrastructural analysis of κOR and ppDYN

Dual immunolabeling using immunoperoxidase to detect ppDYN and immunogold-silver to detect κOR (Fig. 5) showed that single axon terminals exhibiting colocalized κOR and ppDYN. Of the 477 κOR-labeled axon terminals examined, 47% (223/477) were dually labeled with ppDYN. Of the ppDYN-labeled axon terminals examined, 42% (223/535) were also immunolabeled with κOR. Of the 223 κOR and ppDYN dual-labeled axon terminals that targeted dendrites 53% (118/223) exhibited asymmetric synapses (Figure 5A,D–E) and 10% (23/223) exhibited symmetric synapses (Fig. 5B). About 37% (83/223) did not form recognizable synaptic contact (Fig. 5C). Many κOR and ppDYN dual-labeled axon terminals contained dense core vesicles (Figure 5D–E).

DISCUSSION

In the present study, we provide neuroanatomical evidence for the targeting of κORs in TH-containing somatodendritic processes in the LC. We also demonstrate, using electron microscopy, that κOR immunoreactivity is present on the cell surface of axon terminals that contain heterogeneous types of synaptic vesicles that primarily form Type I (asymmetric-type) synapses with postsynaptic targets. A subset of κOR immunoreactive axon terminals exhibit ppDYN immunoreactivity and these are also primarily of the excitatory-type. In summary, the present findings provide an anatomical substrate for direct targeting of κORs in noradrenergic neurons as well as a complex pre-synaptic organization with κORs acting, in part, as autoreceptors that may modulate release of DYN from LC afferents.

Methodological considerations

A caveat inherent to pre-embedding dual immunolabeling approaches is related to limited and/or differential penetration of immunoreagents in thick tissue sections. Limited penetration of κOR/ppDYN antibodies may result in an underestimation of the relative frequencies of their distributions. Likewise, limited penetration of the TH antiserum, may result in underestimation of the number of synapses found on TH-labeled dendrites, particularly in distal dendrites in the LC region sampled. This limitation was minimized by collecting tissue sections near the tissue-Epon interface where penetration is optimal and sampling profiles only when both markers (e.g. κOR+TH or κOR+ppDYN) were clearly present in fields included for analysis (Leranth and Pickel, 1989).

κOR distribution in the LC

DYN is considered to be a selective endogenous ligand of the κOR (Chavkin et al., 1982). Though there are some reports that this endogenous opioid has some affinity for mu opioid receptors (Mulder et al., 1989), it has been shown that DYN has 100 times greater affinity for κOR (Zhang et al., 1998). Additional members of the opioid receptor family have been well characterized in the LC (Mansour et al., 1994a). For example, mu opioid receptors are predominantly localized to the plasma membrane of LC neurons (Van Bockstaele et al., 1996) while delta opioid receptors are localized primarily to pre-synaptic sites in the LC where they are associated with the membranes of large dense core vesicles (Van Bockstaele et al., 1997).

In the present study, κORs were identified in both pre- and post-synaptic profiles with a greater preponderance in axon terminals. The more prominent localization of κOR in axon

terminals suggests that this endogenous opioid system may be poised to modulate afferent drive in this region as suggested by our and others' electrophysiological studies (Kreibich et al., in press). This is consistent with reports of κOR targeting in other CNS regions (Arvidsson et al., 1995; DePaoli et al., 1994; Hoshi et al., 1996; Hoshi et al., 1997; Mansour et al., 1994a). For example, in rat spinal cord, κOR was commonly localized to dendrites, axons, axon terminals and less commonly to glia and somata (Harris et al., 2004). In the present study, we showed a preponderance of κOR localization in axon terminals compared to dendritic localization. Previous electrophysiological studies examining κORs have suggested that modulation of this receptor influences pre-synaptic transmitter release. The present findings are also consistent with recent studies showing that in the ventral tegmental area modulation of κORs can suppress dopamine release via pre- and postsynaptic actions of κOR selective agonists (Ford et al., 2007).

κOR-labeled axon terminals contained both small clear vesicles and large dense core vesicles and often formed asymmetric synaptic specializations while some κOR-labeled axon terminals formed symmetric synaptic contacts with noradrenergic dendrites in the LC. Asymmetric synapses are thought to be involved in excitatory neurotransmission whereas symmetric synapses are thought to be involved in inhibitory neurotransmission (Gray, 1959; Peters and Palay, 1996; Peters et al., 1991). Using ultrastructural analysis, we showed that the majority of DYN-labeled axon terminals form asymmetric synapses with TH-labeled dendrites (Reyes et al., 2007). The evidence of κOR-labeled axon terminals targeting noradrenergic LC dendrites defines the site of action of DYN. We have demonstrated that vesicular glutamate transporter-1 (VGlut)-labeled terminals contain DYN in LC and more often these terminals form asymmetric synapse with unidentified dendrites (Barr and Van Bockstaele, 2005). This is further supported by our recent findings showing that axon terminals containing κOR were co-localized with VGlut which often form asymmetric synaptic specializations with unlabeled dendrites (Kreibich et al., 2008). These data suggest that DYN is likely a co-transmitter in glutamatergic axons that to some extent directly synapse on noradrenergic neurons in the LC. In addition, κOR in DYN-immunoreactive or in non-immunoreactive terminals could modulate glutamate release. Previous studies have shown that kappa opioid agonists decrease evoked excitatory postsynaptic potentials in the LC (Pinnock, 1992). Taken together, these observations raise the possibility that DYN has presynaptic effects in modulating glutamatergic neurotransmission in the LC.

Our recent results also revealed that κOR-labeled axon terminals exhibited CRF immunoreactivity (Kreibich et al., 2008). Almost 50% of the κOR+CRF dual-labeled axon terminals formed identifiable synapses. The majority of these identifiable synapses form asymmetric synapses with unlabeled dendrites. The co-localization of κOR-labeled axon terminal with either VGlut or CRF is consistent with the presynaptic modulation of glutamatergic and CRF afferents to the LC.

The present study also demonstrates that κOR and ppDYN are colocalized in the same axon terminals. Based on binding studies and bioassays, DYN is an endogenous ligand for κOR (Chavkin et al., 1982). Thus, it is likely that in the κOR and ppDYN-dual labeled axon terminals, κOR may serve as autoreceptors that regulate the presynaptic release of DYN that in turn regulates LC activity.

Some κOR-labeled axon terminals did not form recognizable synapses in the plane of section analyzed. These κOR-labeled axon terminals may have formed synapses in another plane or they may arise from other neuromodulatory afferents that do not readily form distinguishable synaptic specializations (Satoh et al., 1982). Although κOR-labeled axon terminals frequently contacted TH-labeled dendrites, there were profiles that also contacted dendrites that lacked TH immunolabeling. This data suggests that κOR may target non-

catecholaminergic neurons in the LC. Identifying the populations of non-catecholaminergic neurons will require dual labeling with other specific neurochemical markers.

The κOR immunoreactivity was also identified along the extrasynaptic portions of the plasma membrane of TH-labeled dendrites and was not commonly associated with the synaptic junction. It has been reported that high levels of κOR mRNA and κOR binding are expressed in LC (Mansour et al., 1994b). The localization of κOR in LC dendrites also suggests the possibility that κORs are positioned to modulate postsynaptic signaling in LC neurons. In the present study, we restricted our analysis to portion of the neuropil known to be enriched with noradrenergic perikarya and dendrites.

Functional implications

LC neurons play an important role in adaptive responses to stress (Aston-Jones et al., 1991). Following stress or in animal models of depression, DYN has been shown to be significantly increased in limbic brain regions (Shirayama et al., 2004). Interestingly, the therapeutic potential of using κOR antagonist for the treatment of depression has been demonstrated (Mague et al., 2003; Shirayama et al., 2004). Microinfusion of the κOR agonist, U50488, into the LC did not alter spontaneous discharge but significantly attenuated phasic discharge evoked by stimuli that engage excitatory amino acid afferents to the LC including, sciatic nerve stimulation and auditory stimuli, and the tonic activation associated with opiate withdrawal (Kreibich et al., 2008). In addition, the κOR agonist also significantly attenuated tonic LC activation by hypotensive stress, an effect mediated by CRF afferents. Intracoerulear microinfusion of the κOR antagonist, nor BNI, prevented the inhibitory effects of U50488 on LC evoke activity (Kreibich et al., 2008). These results suggest that κOR agonists are poised to presynaptically inhibit diverse signaling to LC neurons. Consistent with previous reports that κORs are positioned to influence both pre- and postsynaptic neurotransmission (Harris et al., 2004), the results of the present study provide a potential mechanism by which κOR and DYN may modulate the activity of LC neurons during stress. Thus, κOR may elicit its actions in the LC via both pre- and postsynaptic effects. Moreover, κORs in LC neurons may also serve as autoreceptors for DYN that may modulate its release.

Acknowledgments

National Institutes of Health; Grant number: DA 09082 (E. J. V. B.)

References

Arvidsson U, Riedl M, Chakrabarti S, Vulchanova L, Lee JH, Nakano AH, Lin X, Loh HH, Law PY, Wessendorf MW, Elde R. The kappa-opioid receptor is primarily postsynaptic: combined immunohistochemical localization of the receptor and endogenous opioids. Proc Natl Acad Sci USA. 1995; 92:5062–5066. [PubMed: 7539141]

Aston-Jones G, Bloom FE. Activity of norepinephrine-containing locus coeruleus neurons in behaving rats anticipates fluctuations in the sleep-waking cycle. J Neurosci. 1981; 1:876–886. [PubMed: 7346592]

Aston-Jones, G.; Foote, SL.; Bloom, FE. Anatomy and physiology of locus coeruleus neurons: functional implications. In: Ziegler, M.; Lake, CR., editors. Norepinephrine (Frontiers of Clinical Neuroscience). Baltimore: Williams and Wilkins; 1984. p. 92-116.

Aston-Jones G, Shipley MT, Chouvet G, Ennis M, Van Bockstaele E, Pieribone V, Shiekhattar R, Akaoka H, Drolet G, Astier B. Afferent regulation of locus coeruleus neurons: anatomy, physiology and pharmacology. Prog Brain Res. 1991; 88:47–75. [PubMed: 1687622]

Barr J, Van Bockstaele EJ. Vesicular glutamate transporter-1 colocalizes with endogenous opioid peptides in axon terminals of the rat locus coeruleus. Anat Rec A Discov Mol Cell Evol Biol. 2005; 284:466–474. [PubMed: 15803474]

Chan J, Aoki C, Pickel VM. Optimization of differential immunogold-silver and peroxidase labeling with maintenance of ultrastructure in brain sections before plastic embedding. J Neurosci Methods. 1990; 33:113–127. [PubMed: 1977960]

Chavkin C, James IF, Goldstein A. Dynorphin is a specific endogenous ligand of the kappa opioid receptor. Science. 1982; 215:413–415. [PubMed: 6120570]

DePaoli AM, Hurley KM, Yasada K, Reisine T, Bell G. Distribution of kappa opioid receptor mRNA in adult mouse brain: an in situ hybridization histochemistry study. Mol Cell Neurosci. 1994; 5:327–335. [PubMed: 7804602]

Drake CT, Patterson TA, Simmons ML, Chavkin C, Milner TA. Kappa opioid receptor-like immunoreactivity in guinea pig brain: ultrastructural localization in presynaptic terminals in hippocampal formation. J Comp Neurol. 1996; 370:377–395. [PubMed: 8799863]

Elam M, Svensson TH, Thoren P. Differentiated cardiovascular afferent regulation of locus coeruleus neurons and sympathetic nerves. Brain Res. 1985; 358:77–84. [PubMed: 4075133]

Elam M, Thoren P, Svensson TH. Locus coeruleus neurons and sympathetic nerves: activation by visceral afferents. Brain Res. 1986; 375:117–125. [PubMed: 3719350]

Elam M, Yao T, Svensson TH, Thoren P. Regulation of locus coeruleus neurons and splanchnic, sympathetic nerves by cardiovascular afferents. Brain Res. 1984; 290:281–287. [PubMed: 6692144]

Elde, R.; Hokfelt, T. Coexistence of opioid peptides with other neurotransmitters. In: Herz, A., editor. Handbook of Experimental Pharmacology, Opioids I. Berlin: Springer; 1993. p. 585-624.

Fallon JH, Leslie FM. Distribution of dynorphin and enkephalin peptides in the rat brain. J Comp Neurol. 1986; 249:293–336. [PubMed: 2874159]

Foote SL, Bloom FE, Aston-Jones G. Nucleus locus ceruleus: new evidence of anatomical and physiological specificity. Physiol Rev. 1983; 63:844–914. [PubMed: 6308694]

Ford CP, Beckstead MJ, Williams JT. Kappa opioid inhibition of somatodendritic dopamine inhibitory postsynaptic currents. J Neurophysiol. 2007; 97:883–891. [PubMed: 17122312]

Goldstein A, Ghazarossian VE. Immunoreactive dynorphin in pituitary and brain. Proc Natl Acad Sci USA. 1980; 77:6207–6210. [PubMed: 6108564]

Gray EG. Axosomatic and axo-dendritic synapses of the cerebral cortex: an electron microscopic study. J Anat. 1959; 93:420–433. [PubMed: 13829103]

Harris JA, Chang PC, Drake CT. Kappa opioid receptors in rat spinal cord: sex-linked distribution differences. Neuroscience. 2004; 124:879–890. [PubMed: 15026128]

Hollt V, Haarmann I, Bovermann K, Jerlicz M, Herz A. Dynorphin-related immunoreactive peptides in rat brain and pituitary. Neurosci Lett. 1980; 18:149–153. [PubMed: 7052485]

Hoshi K, Ma T, Ho IK. Precipitated kappa-opioid receptor agonist withdrawal increase glutamate in rat locus coeruleus. Eur J Pharmacol. 1996; 314:301–306. [PubMed: 8957250]

Hoshi K, Ma T, Oh S, Ho IK. Increased release of excitatory amino acids in rat locus coeruleus in kappa-opioid agonist dependent rats precipitated by nor-binaltorphimine. Brain Res. 1997; 753:63–68. [PubMed: 9125432]

Khachaturian H, Watson SJ, Lewis ME, Coy D, Goldstein A, Akil H. Dynorphin immunocytochemistry in the rat central nervous system. Peptides. 1982; 3:941–954. [PubMed: 6132365]

Kreibich AS, Reyes BAS, Curtis AL, Ecke L, Chavkin C, Van Bockstaele EJ, Valentino RJ. Presynaptic inhibition of diverse afferents to the locus coeruleus by kappa opiate receptors: a novel mechanism for regulating the central norepinephrine system. J Neurosci. 2008; 28:6516–6525. [PubMed: 18562623]

Lechner SM, Curtis AL, Brons R, Valentino RJ. Locus coeruleus activation by colon distention: role of corticotropin-releasing factor and excitatory amino acids. Brain Res. 1997; 756:114–124. [PubMed: 9187321]

Leranth, C.; Pickel, VM. Electron microscopic preembedding double-labeling methods. In: Heimer, L.; Zaborszky, L., editors. Neuroanatomical tracing methods 2. 1. New York: Plenum Press; 1989. p. 129-172.

Mague SD, Pliakas AM, Todtenkopf MS, Tomasiewicz HC, Zhang Y, Stevens WC Jr, Jones RM, Portoghese PS, Carlezon WA Jr. Antidepressant-like effects of kappa-opioid receptor antagonists in the forced swim test in rats. J Pharmacol Exp Ther. 2003; 305:323–330. [PubMed: 12649385]

Mansour A, Fox CA, Burke S, Meng F, Thompson RC, Akil H, Watson SJ. Mu, delta, and kappa opioid receptor mRNA expression in the rat CNS: an in situ hybridization study. Journal of Comparative Neurology. 1994a; 350:412–438. [PubMed: 7884049]

Mansour A, Fox CA, Meng F, Akil H, Watson SJ. Kappa 1 receptor mRNA distribution in the rat CNS: comparison to kappa receptor binding and prodynorphin mRNA. Mol Cell Neurosci. 1994b; 5:124–144. [PubMed: 8032682]

McCormick DA, Pape HC, Williamson A. Actions of norepinephrine in the cerebral cortex and thalamus: implications for function of the central noradrenergic system. Prog Brain Res. 1991; 88:293–305. [PubMed: 1726028]

McFadzean I, Lacey MG, Hill RG, Henderson G. Kappa opioid receptor activation depresses excitatory synaptic input to rat locus coeruleus neurons in vitro. Neuroscience. 1987; 20:231–239. [PubMed: 3031541]

McLaughlin JP, Marton-Popovici M, Chavkin C. Kappa opioid receptor antagonism and prodynorphin gene disruption block stress-induced behavioral responses. J Neurosci. 2003; 23:5674–5683. [PubMed: 12843270]

Miyawaki T, Kawamura H, Komatsu K, Yasugi T. Chemical stimulation of the locus coeruleus: inhibitory effects on hemodynamics and renal sympathetic nerve activity. Brain Res. 1991; 568:101–108. [PubMed: 1687667]

Morilak DA, Fornal CA, Jacobs BL. Effects of physiological manipulations on locus coeruleus neuronal activity in freely moving cats. I. Thermoregulatory challenge. Brain Res. 1987a; 422:17–23. [PubMed: 3676779]

Morilak DA, Fornal CA, Jacobs BL. Effects of physiological manipulations on locus coeruleus neuronal activity in freely moving cats. II. Cardiovascular challenge. Brain Res. 1987b; 422:24–31. [PubMed: 3676783]

Mulder AH, Wardeh G, Hogenboom F, Frankhuyzen AL. Selectivity of various opioid peptides towards delta-, kappa; and mu-opioid receptors mediating presynaptic inhibition of neurotransmitter release in the brain. Neuropeptides. 1989; 14:99–104. [PubMed: 2573000]

Murase S, Takayama M, Nosaka S. Chemical stimulation of the nucleus locus coeruleus: cardiovascular responses and baroreflex modification. Neurosci Lett. 1993; 153:1–4. [PubMed: 8099722]

Peters A, Palay SL. The morphology of synapses. J Neurocytol. 1996; 25:687–700. [PubMed: 9023718]

Peters, A.; Palay, SL.; Webster, Hd. The Fine Structure of the Nervous System. New York: Oxford University Press; 1991.

Pfeiffer A, Brantl V, Herz A, Emrich HM. Psychotomimesis mediated by kappa opiate receptors. Science. 1986; 233:774–776. [PubMed: 3016896]

Pinnock RD. A highly selective kappa-opioid receptor agonist, CI-977, reduces excitatory synaptic potentials in the rat locus coeruleus in vitro. Neuroscience. 1992; 47:87–94. [PubMed: 1315940]

Reyes BAS, Drolet G, Van Bockstaele EJ. Dynorphin and stress-related peptides in rat locus coeruleus: contribution of amygdalar efferents. J Comp Neurol. 2008; 508:663–675. [PubMed: 18381633]

Reyes BAS, Johnson AD, Glaser JD, Commons KG, Van Bockstaele EJ. Dynorphin-containing axons directly innervate noradrenergic neurons in the rat nucleus locus coeruleus. Neuroscience. 2007; 145:1077–1086. [PubMed: 17289275]

Roth BL, Baner K, Westkaemper R, Siebert D, Rice KC, Steinberg S, Ernsberger P, Rothman RB. Salvinorin A: a potent naturally occurring nonnitrogenous kappa opioid selective agonist. Proc Natl Acad Sci USA. 2002; 99:11934–11939. [PubMed: 12192085]

Satoh K, Kashiba A, Kimura H, Maeda T. Noradrenergic axon terminals in the substantia gelatinosa of the rat spinal cord: an electron-microscopic study using glyoxylic acid-potassium permanganate fixation. Cell Tissue Res. 1982; 222:359–378. [PubMed: 7083306]

Schenk S, Partridge B, Shippenberg TS. U69593, a kappa-opioid agonist, decreases cocaine self-administration and decreases cocaine-produced drug-seeking. Psychopharmacology (Berl). 1999; 144:339–346. [PubMed: 10435406]

Shirayama Y, Ishida H, Iwata M, Hazama GI, Kawahara R, Duman RS. Stress increases dynorphin immunoreactivity in limbic brain regions and dynorphin antagonism produces antidepressant-like effects. J Neurochem. 2004; 90:1258–1268. [PubMed: 15312181]

Svensson TH. Peripheral, autonomic regulation of locus coeruleus noradrenergic neurons in brain: putative implications for psychiatry and psychopharmacology. Psychopharmacology (Berl). 1987a; 92:1–7. [PubMed: 3110818]

Svensson TH. Stress, central neurotransmitters, and the mechanism of action of alpha 2-adrenoceptor agonists. J Cardiovasc Pharmacol. 1987b; 10(Suppl 12):S88–92. [PubMed: 2455197]

Todtenkopf MS, Marcus JF, Portoghese PS, Carlezon WA Jr. Effects of kappa-opioid receptor ligands on intracranial self-stimulation in rats. Psychopharmacology (Berl). 2004; 172:463–470. [PubMed: 14727002]

Valentino, RJ.; Curtis, AL.; Page, ME.; Pavcovich, LA.; Lechner, SM.; Van Bockstaele, EJ. The locus coeruleus-noradrenergic system as an integrator of stress responses. In: Morrison, AR.; Fluharty, SJ., editors. Progress in Psychobiology and Physiological Psychology. San Diego, CA: Academic Press; 1998. p. 91-126.

Valentino RJ, Foote SL, Aston-Jones G. Corticotropin-releasing factor activates noradrenergic neurons of the locus coeruleus. Brain Res. 1983; 270:363–367. [PubMed: 6603889]

Van Bockstaele EJ, Colago EEO, Moriwaki A, Uhl GR. Mu-opioid receptor is located on the plasma membrane of dendrites that receive asymmetric synapses from axon terminals containing leucine-enkephalin in the rat nucleus locus coeruleus. Journal of Comparative Neurology. 1996; 376:65–74. [PubMed: 8946284]

Van Bockstaele EJ, Commons K, Pickel VM. Delta-opioid receptor is present in presynaptic axon terminals in the rat nucleus locus coeruleus: relationships with methionine5-enkephalin. Journal of Comparative Neurology. 1997; 388:575–586. [PubMed: 9388017]

Van Bockstaele EJ, Pickel VM. Ultrastructure of serotonin-immunoreactive terminals in the core and shell of the rat nucleus accumbens: cellular substrates for interactions with catecholamine afferents. J Comp Neurol. 1993; 334:603–617. [PubMed: 8408768]

Wang Y, Xui W, Chavkin C, Van Bockstaele EJ, Liu-Chen L-Y. Effects of agonists on subcellular distribution of kappa opioid receptor in rat spinal cord. Soc Neurosci Abstr. 2007; 353.2:G27.

Waterhouse BD, Border B, Wahl L, Mihailoff GA. Topographic organization of rat locus coeruleus and dorsal raphe nuclei: distribution of cells projecting to visual system structures. J Comp Neurol. 1993; 336:345–361. [PubMed: 8263226]

Watson SJ, Khachaturian H, Akil H, Coy DH, Goldstein A. Comparison of the distribution of dynorphin systems and enkephalin systems in brain. Science. 1982; 218:1134–1136. [PubMed: 6128790]

Watson SJ, Khachaturian H, Taylor L, Fischli W, Goldstein A, Akil H. Pro-dynorphin peptides are found in the same neurons throughout rat brain: immunocytochemical study. Proc Natl Acad Sci USA. 1983; 80:891–894. [PubMed: 6131416]

Zhang S, Tong Y, Tian M, Dehaven RN, Cortesburgos L, Mansson E, Simonin F, Kieffer B, Yu L. Dynorphin A as a potential endogenous ligand for four members of the opioid receptor gene family. J Pharmacol Exp Ther. 1998; 286:136–141. [PubMed: 9655852]

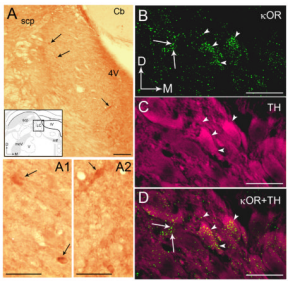

Figure 1.

A. Brightfield photomicrograph showing immunoperoxidase labeling for kappa opioid receptors (κOR) in the locus coeruleus (LC). Shown in panel A is an inset of a schematic diagram adapted from the rat brain atlas of Swanson (1992) depicting the region shown in panel A as well as the area targeted for ultrastructural analysis. Arrows point to peroxidase immunoreactivity indicative of κOR in cell bodies that can be seen at higher magnification photomicrograph in A1. Double arrows indicate κOR immunoreactivity in cell bodies that can seen at higher magnification in A2. In the inset, arrows indicate the dorsal (D) and medial (M) orientation of the section illustrated. **B**–**D.** Confocal fluorescence photomicrographs of κOR labeled with fluorescein isothiocyanate (green) and tyrosine hydroxylase (TH) labeled with rhodamine isothiocyanate (pseudocolored in magenta) in the LC. Arrowheads in panel B point to κOR that can also be seen in the merged image in panel D. Arrows in panels B and D point to some κOR labeled processes. Arrowheads in panel C point to TH neurons that are also seen in the merged image in panel D. Arrows indicate the dorsal (D) and medial (M) orientation of the tissue section. Abbreviations: scp, superior cerebellar peduncle; D, dorsal; 4V, fourth ventricle; M, medial; mlf, medial longitudinal fasciculus; moV, motor root of the trigeminal nucleus; V, motor nucleus of the trigeminal nucleus. Scale bars, 100 μm (AD), 25 μm (A1 and A2).

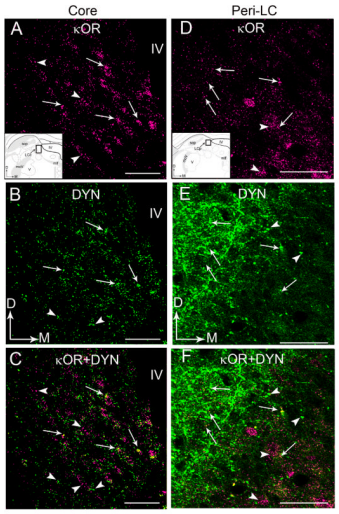

Figure 2.

Confocal fluorescence photomicrographs showing κOR and DYN immunoreactivities in coronal sections through the core (A–C) and peri-LC (D–F). **A and D.**κOR immunolabeling was detected by rhodamine isothiocyanate (pseudocolored in magenta). Arrows point to individual DYN-varicose processes that contain κOR. Arrowheads point to varicose processes that only contain κOR. Insets show schematic diagrams adapted from the rat brain atlas of Swanson (1992) depicting the core (LCc) and peri-LC (LCp) regions sampled. In the insets, arrows indicate dorsal (D) and medial (M) orientation of the sections illustrated. Abbreviations: scp, superior cerebellar peduncle; D, dorsal; IV, fourth ventricle; M, medial; mlf, medial longitudinal fasciculus; moV, motor root of the trigeminal nucleus; V, motor nucleus of the trigeminal nucleus. **B and E.** DYN was detected by fluorescein isothiocyanate (green). Arrows point to individual DYN-varicose processes that contain κOR. Arrowheads point to varicose processes that only contain DYN. **C and F.** Merged images. Arrows point to κOR- and DYN-dual labeled varicose processes. Arrowheads to either κOR- or DYN-labeled varicose processes. Abbreviation: IV, fourth ventricle. Scale bar, 100 μm.

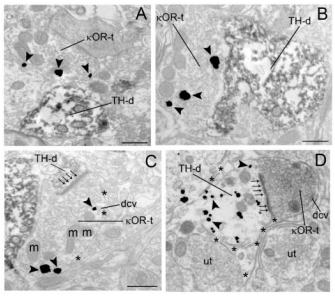

Figure 3.

Electron photomicrographs showing synaptic contacts formed by κOR-labeled axon terminals with TH-labeled dendrites in the locus coeruleus (LC). **A.** An immunoperoxidase-labeled TH dendrite (TH-d) and an immunogold-silver labeled (arrowheads) κOR terminal (κOR-t) are seen in the same field. **B**–**C.** Axon terminals exhibiting immunogold-silver labeling (arrowheads) for κOR (κOR-t) target dendrites containing immunoperoxidase-labeling for TH (TH-d). In panel C, the κOR-t forms an asymmetric-type synapse (small arrows) with a TH-labeled dendrite (TH-d). **D.** An immunoperoxidase-labeled κOR terminal (κOR-t) forms an asymmetric synapse (small arrows) with an immunogold-labeled (arrowheads) TH dendrite (TH-d) surrounded by an astrocytic process (asterisks). Abbreviation: m, mitochondria; ut, unlabeled terminal. Scale bars, 0.5μm.

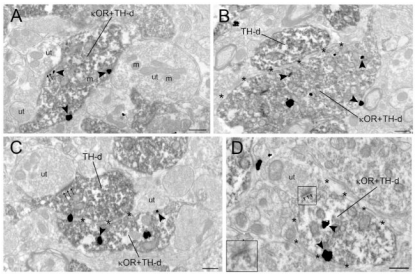

Figure 4.

Electron photomicrographs showing immunoperoxidase labeling for TH and immunogold-silver labeling for κOR in the locus coeruleus (LC). **A.** A dendrite contains immunogold-silver labeling (arrowheads) for κOR. The dually labeled dendrite (κOR+TH-d) receives an asymmetric (small arrows) synapse from an unlabeled terminal (ut). **B.** Two adjacent TH-labeled dendrites (TH-d) exhibiting immnoperoxidase labeling are separated by an astrocytic process (asterisks). One of these TH-labeled dendrites also exhibits immunogold-silver labeling (arrowheads) for κOR (κOR+TH-d). **C.** Two adjacent TH-labeled dendrites (TH-d) exhibiting immnoperoxidase labeling are separated by an astrocytic process (asterisks). One of these TH-labeled dendrites also exhibits immunogold-silver labeling (arrowheads) for κOR (κOR+TH-d). This κOR+TH-dual labeled dendrite forms an “undefined” association with unlabeled terminal (ut). A TH-labeled dendrite receives an asymmetric synapse (small arrows) from an unlabeled terminal (ut) containing several mitochondria (m). Also shown are other TH-labeled dendrites in the neuropil. **D.** A κOR+TH-d receives an asymmetric synapse (small arrows) from an unlabeled terminal (ut) and is surrounded by an astrocytic process (asterisks). Inset shows the higher magnification of the boxed area. m, mitochondria. Scale bars, 0.5μm.

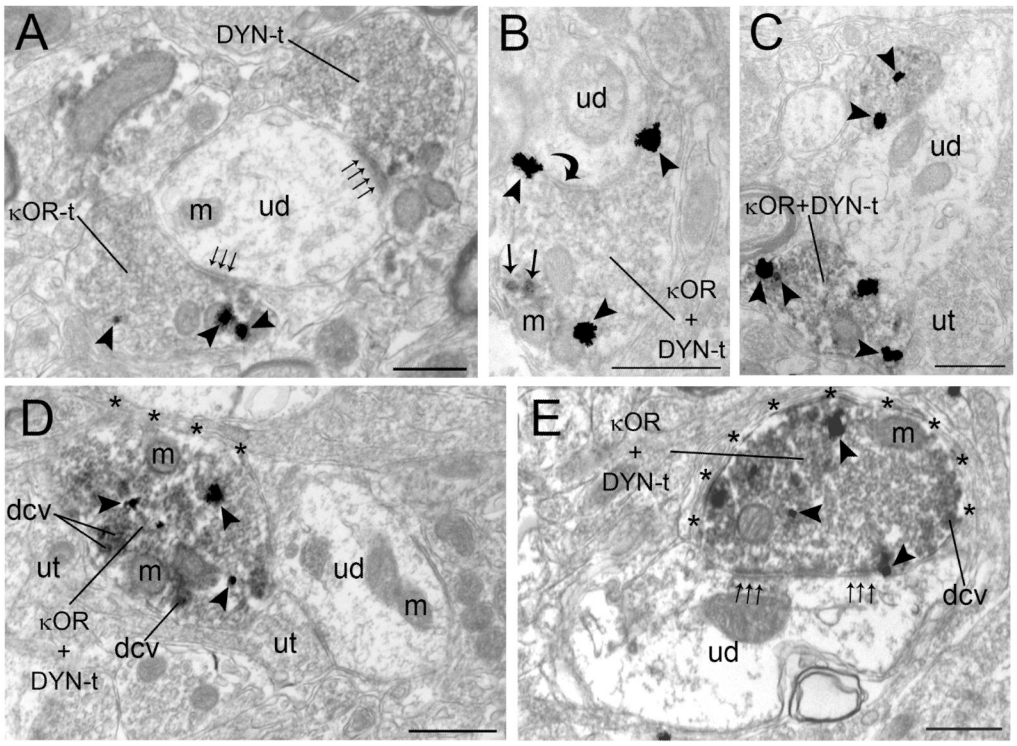

Figure 5.

Ultrastructural evidence for convergence and co-localization of κOR and DYN in the locus coeruleus (LC). **A.** An immunogold-silver labeled (arrowheads) κOR terminal (κOR-t) and an immunoperoxidase-labeled DYN axon terminal (DYN-t) form asymmetric (small arrows) synapse with a common unlabeled dendrite (ud). **B.** An axon terminal containing both immunoperoxidase labeling for DYN (arrows) and immunogold-silver labeling (arrowheads) for κOR (κOR+DYN-t) forms a symmetric synapse (curved arrow) with unlabeled dendrite (ud). **C.** Two axon terminals, containing both immunoperoxidase labeling for DYN and immunogold-silver labeling (arrowheads) for κOR (κOR+DYN-t), contact an unlabeled dendrite (ud). **D**–**E.** Axon terminals dually labeled for κOR and DYN-t (κOR +DYN-t) are directly apposed to unlabeled dendrites. Both dually labeled κOR+DYN terminals contain dense core vesicles (dcv). In panel D, the κOR+DYN-t does not form an identifiable synapse whereas in panel E, the κOR+DYN-t forms a perforated synapse consistent with an asymmetric type (small arrows) synaptic specialization with unlabeled dendrite (ud). These axon terminals are also surrounded with astrocytic processes (asterisks). Also shown are unlabeled terminals. m, mitochondria. Scale bars, 0.5μm.

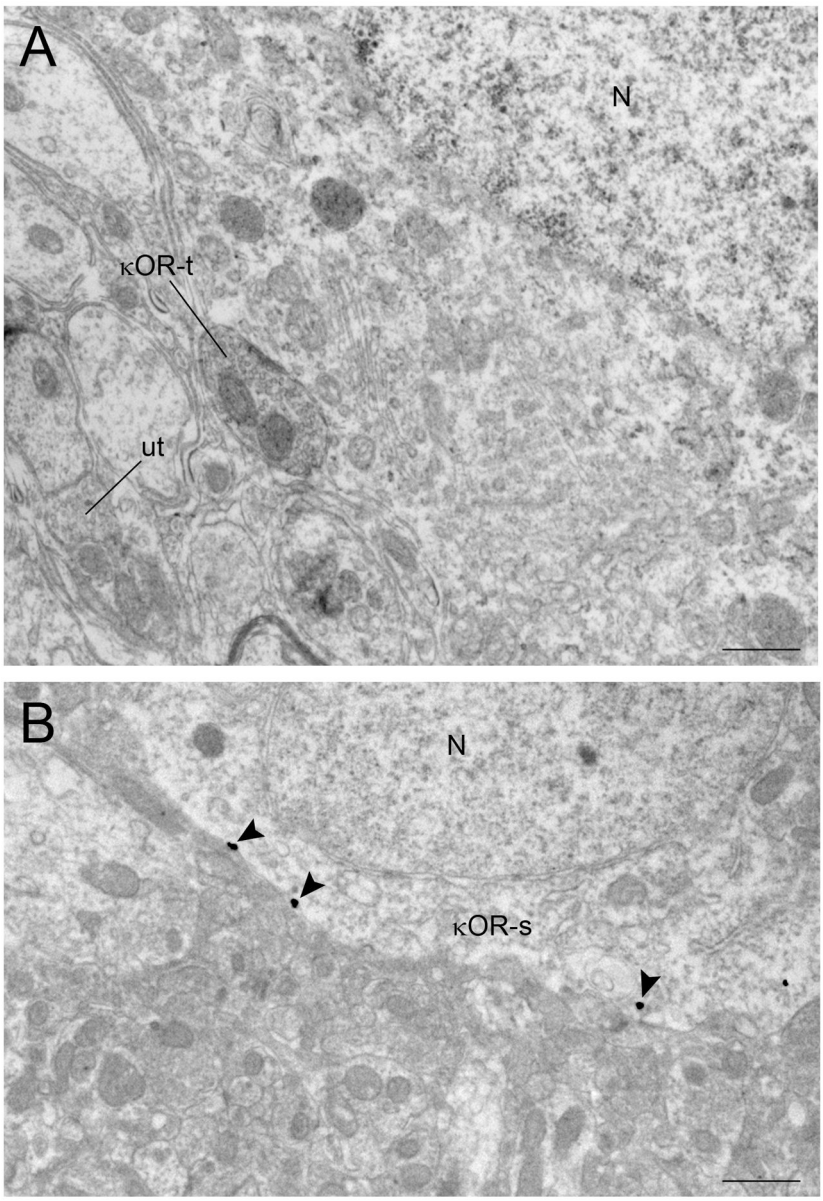

Figure 6.
Electron photomicrographs showing κOR immunoreactivity in cell bodies in the locus coeruleus (LC). **A.** An immunoperoxidase-labeled κOR axon terminal (κOR-t) is contacting a perikaryon. **B.** Immunogold-silver labeling for κOR (arrowheads) is present in a perikaryon in the LC. N, nucleus. Scale bars, 0.5μm